Journal of Experimental Botany, Vol. 64, No. 10, pp. 2817–2829, 2013
doi:10.1093/jxb/ert125 Advance Access publication 16 May, 2013
This paper is available online free of all access charges (see http://jxb.oxfordjournals.org/open_access.html for further details)

Journal of Experimental Botany
www.jxb.oxfordjournals.org

RESEARCH PAPER

ARA7(Q69L) expression in transgenic *Arabidopsis* cells induces the formation of enlarged multivesicular bodies

Tianran Jia[1], Caiji Gao[1], Yong Cui[1], Junqi Wang[1], Yu Ding[1], Yi Cai[1], Takashi Ueda[2], Akihiko Nakano[2,3] and Liwen Jiang[1,*]

[1] School of Life Sciences, Centre for Cell and Developmental Biology, The Chinese University of Hong Kong, Shatin, New Territories, Hong Kong, China
[2] Department of Biological Sciences, Graduate School of Science, The University of Tokyo, Bunkyo-ku, Tokyo 113-0033, Japan
[3] Molecular Membrane Biology Laboratory, RIKEN Advanced Science Institute, Wako, Saitama 351-0198, Japan

*To whom correspondence should be addressed. E-mail: ljiang@cuhk.edu.hk

Received 9 March 2013; Revised 10 April 2013; Accepted 12 April 2013

Abstract

***Arabidopsis thaliana* ARA7 (*At*RabF2b), a member of the plant Rab5 small GTPases functioning in the vacuolar transport pathway, localizes to pre-vacuolar compartments (PVCs), known as multivesicular bodies (MVBs) in plant cells. Overexpression of the constitutively active GTP-bound mutant of ARA7, ARA7(Q69L), induces the formation of large ring-like structures (1–2 μm in diameter). To better understand the biology of these ARA7(Q69L)-induced ring-like structures, transgenic *Arabidopsis* cell lines expressing ARA7(Q69L) tagged with green fluorescent protein (GFP) under the control of a heat shock-inducible promoter were generated. In these transgenic cells, robust ring-like structures were formed after 4 h of heat shock induction. Transient co-expression, confocal imaging, and immunogold electron microscopy (immunogold-EM) experiments demonstrated that these GFP–ARA7(Q69L)-labelled ring-like structures were distinct from the Golgi apparatus and *trans*-Golgi network, but were labelled with an antibody against an MVB marker protein. In addition, live cell imaging and detailed EM analysis showed that the GFP–ARA7(Q69L)-induced spherical structures originated from the homotypic fusion of MVBs. In summary, it was demonstrated that GFP–ARA7(Q69L) expression is an efficient tool for studying PVC/MVB-mediated protein trafficking and vacuolar degradation in plant cells.**

Key words: ARA7(Q69L), homotypic fusion, MVB enlargement, multivesicular body, pre-vacuolar compartment, transgenic *Arabidopsis* cells.

Introduction

In plant cells, protein sorting to the vacuole in the secretory pathway begins at the rough endoplasmic reticulum (ER) and then proceeds through the Golgi apparatus and post-Golgi compartments, known as the *trans*-Golgi network (TGN) and the pre-vacuolar compartment (PVC) or multivesicular body (MVB) (Foresti and Denecke, 2008). The plant MVB, a membrane-bound organelle containing internal vesicles, is believed to be the structural equivalent of the mammalian late endosome and serves as the last sorting station before cargo reaches the vacuole (Jiang and Rogers, 1998; Tse *et al*., 2004; Scheuring *et al*., 2011).

Membrane trafficking between different organelles is regulated by Rab small GTPases. Different Rab proteins localize to distinct membrane domains and function in specific trafficking steps (Woollard and Moore, 2008; Segev, 2011). The *Arabidopsis thaliana* genome contains 57 Rab members, which can be grouped into eight classes (Vernoud *et al*., 2003). Of these, the RabF family, also known as the Rab5 family, localizes to MVBs and plays a critical role in vacuolar trafficking (Sohn *et al*., 2003; Lee *et al*., 2004; Haas *et al*., 2007). Three Rab5 homologues have been identified in *Arabidopsis*, namely ARA7 (*At*RabF2b), RHA1 (*At*RabF2a) and ARA6 (*At*RabF1). They exhibit high

sequence similarity to mammalian Rab5 and yeast Ypt51 (Bucci *et al*., 1992; Singer-Kruger *et al*., 1995). In *Arabidopsis*, ARA6, the only plant-unique myristoylated Rab5 protein, functions in the trafficking from endosomes to the plasma membrane, and may also be involved in vacuolar trafficking and salinity stress response (Ueda *et al*., 2001; Ebine *et al*., 2011). Likewise, ARA7 also plays a role in endocytic trafficking, as ARA7-positive compartments are enlarged and show ring-like structures in cells in which GNOM, the GDP/GTP exchange factor for Arf GTPases, is mutated (Geldner *et al*., 2003). In addition, there is substantial ultrastructural evidence from confocal and immunogold electron microscopy (immunogold-EM) experiments showing that ARA7 and RHA1 (a conventional Rab5 homologue) localize to PVCs/MVBs and function in the vacuolar trafficking pathway (Sohn *et al*., 2003; Kotzer *et al*., 2004; Lee *et al*., 2004; Haas *et al*., 2007).

Previous studies show that ARA7(Q69L), a constitutively active ARA7 mutant, tagged with green fluorescent protein (GFP) resides on the membranes of ring-like structures and on the tonoplast when expressed in plant cells (Ueda *et al*., 2001; Kotzer *et al*., 2004; Ebine *et al*., 2011). This specific mutation disrupts GTP hydrolysis, thereby leading to a higher proportion of GTP-bound ARA7 proteins and promoting excessive membrane fusion, which results in the accumulation of ring-like structures (Ueda *et al*., 2001; Kotzer *et al*., 2004). Because of their enlarged size, different microdomains can be differentiated easily, and proteins residing on or inside these ring-like structures can be easily viewed by light microscopy (Cai *et al*., 2012; Gao *et al*., 2012). However, before one can use this model of ARA7(Q69L)-induced enlarged sphere formation for future studies, it is first necessary to gain a better understanding of the biology behind these ring-like structures in plant cells.

To begin to achieve this goal, transgenic *Arabidopsis* cell lines expressing GFP–ARA7(Q69L) under the control of a heat shock-inducible promoter (HSP) were generated. Multiple approaches, including transient co-expression, confocal imaging, and immunogold-EM experiments, were performed to demonstrate that these GFP–ARA7(Q69L)-labelled ring-like structures were distinct from the Golgi apparatus and the TGN, but that they were labelled by an MVB marker protein. In addition, live cell imaging and EM analysis showed these spherical structures to be derived largely from the homotypic fusion of MVBs. Therefore, ARA7(Q69L) expression appears to serve as an excellent tool for inducing MVB enlargement and for studying the relative localization of different proteins on MVBs.

Materials and methods

Preparation of constructs

A two-step cloning procedure was used to generate the final construct, which contained the HSP–GFP–ARA7(Q69L) for *Agrobacterium tumefaciens*-mediated transformation of *Arabidopsis* PSBD cells. First, the heat shock promoter (hsp18.2) was excised from the pHGT1 vector (a gift from Dr Karin Schumacher, Heidelberg University) and subcloned into the binary vector pBI121 (Chen *et al*., 2003) using the same restriction sites. Secondly, a cDNA encoding ARA7(Q69L) (a gift from Dr Takashi Ueda, University of Tokyo) was produced using the following primers: 5'-GGGTCTAGAATGGCTGCAGCTGGAAACAAG-3' and 5'-GGGCTCGAGCTAAGCACAACAAGATGAGCTC-3'. Thereafter, PCR-amplified fragments were digested with *Xba*I/*Xho*I and subcloned into the HSP-containing pBI121 vector obtained from the first step using the same restriction sites. All other constructs used for transient expression experiments were derived from plasmids with a pBI221 backbone and containing the *Cauliflower mosaic virus* (CaMV) 35S promoter and the nopaline synthase (NOS) terminator (Miao *et al*., 2008). The authenticity of all constructs was verified by both restriction mapping and DNA sequencing.

Transient expression

Protoplasts derived from *A. thaliana* PSBD cell suspension cultures (ecotype Landsberg *erecta*) were used for transient expression experiments. Plasmid DNA was purified by conventional phenol/chloroform extraction. After electroporation, transfected protoplasts were incubated at 27 °C for 6–12 h before confocal imaging. For each transient expression sample, >80% of successfully transformed protoplasts were showing the typical pattern presented here. Detailed procedures for cell line maintenance and transient expression have been described previously (Miao and Jiang, 2007; Wang *et al*., 2010).

Transformation of Arabidopsis *cells*

The HSP–GFP–ARA7(Q69L)/pBI121 construct was used for *Agrobacterium*-mediated transformation. Transfected cells were grown on Murashige and Skoog (MS) agar (1% agar, w/v) plates containing kanamycin (100 μg ml^{-1}) and cefotaxime sodium (250 μg ml^{-1}) for 3–4 weeks until the formation of transformed colonies. Colonies were transferred to kanamycin-containing plates for further screening. Detailed procedures for the generation of transgenic cell lines have been previously described (Tse *et al*., 2004; Lam *et al*., 2007; Wang *et al*., 2010). Transgenic *Arabidopsis* cell lines were maintained in both liquid and solid cultures supplemented with a lower concentration of kanamycin (50 μg ml^{-1}). Suspension-cultured cells were transferred onto MS plates and cultured for an additional 7–10 d before being used. Transgenic cells were imaged by confocal microscopy 1 h after heat shock treatment at 37 °C and 3–4 h after incubation at 27 °C, respectively.

Dynamic study of GFP fusions in transgenic cells by spinning disc confocal microscopy

Transgenic *Arabidopsis* cells expressing GFP–ARA7(Q69L) were subjected to either a brief heat shock treatment or standard incubation before being observed by confocal microscopy. Images were collected using a Revolution XD spinning disc laser confocal microscopy system (Andor Technology China) fitted with a ×100 oil lens. Three-dimensional time-lapse images were obtained from stacks of 2-D images, which were collected at short intervals (Wang *et al*., 2011). The typical fusion events presented here were readily observed in >80% of the transgenic cells.

Immunofluorescent staining and confocal imaging

Transgenic *Arabidopsis* and wild-type (WT) cells were subjected to heat shock treatment for 1 h at 37 °C before fixation in MS cell culture medium containing 0.5% glutaraldehyde for 15 min at room temperature. After a brief wash with MS medium three times, the cells were treated with MS containing 0.1% pectinase and 1% cellulase for 1 h at 28 °C. Then the cells were washed with phosphate-buffered saline (PBS), and treated with PBS containing 0.1% sodium tetrahydridoborate ($NaBH_4$) at 4 °C overnight. For immunolabelling, polyclonal antibodies against the vacuolar sorting receptor (VSR) (Tse *et al*., 2004), syntaxin of plants 61 (SYP61) (Sanderfoot *et al*., 2001), mannosidase I (ManI) (Li *et al*., 2002), and vacuolar-type

H^+-translocating inorganic pyrophosphatase (VPPase) (Jiang *et al*., 2001) were used at 4 μg ml^{-1} in an overnight incubation at 4 °C. Alexa Fluor-568 anti-rabbit (Molecular Probes, USA) secondary antibody was used for immunofluorescent detection at 1:1000 dilution. Confocal images were collected using an Olympus FluoView FV1000 confocal microscope with a ×60 water lens. The GFP signal was collected with excitation at 488 nm and emission at 500–550 nm using a band-pass filter. Alexa Fluor-568 or mRFP (monomeric red fluorescent protein) signals were collected in another detection channel with excitation at 559 nm and emission at 570–630 nm (band-pass filter). The line sequential scanning mode was always used in dual-channel observations to avoid cross-talk between two channels. All images were prepared using Adobe Photoshop as described before. Detailed protocols for immunolabelling and the settings used to collect the confocal images have been described elsewhere (Paris *et al*., 1996; Jiang and Rogers, 1998; Ritzenthaler *et al*., 2002; Lam *et al*, 2009; Shen *et al*., 2011; Ding *et al*., 2012; Gao *et al*., 2012). These experiments were repeated at least three times, and the typical labelling patterns were observed in each independent experiment.

Electron microscopy

Ultrastructural analysis was performed using 7-day-old transgenic cells grown on MS plates. These cells were subjected to heat shock treatment and then fixed immediately in 25 mM CaCo buffer, pH 7.2 at 22 °C containing 2% glutaraldehyde (v/v) and 10% picric acid (w/v) at 4 °C overnight. After briefly washing with CaCo buffer, cells were incubated in a second fixative [25 mM CaCo buffer, pH 7.2 at 22 °C containing 2% osmium tetroxide (w/v) and 0.5% potassium ferricyanide (w/v)], followed by dehydration, infiltration, and embedding in Spurr's resin. For high-pressure freezing/freeze substitution (HPF), the cells were frozen in a high-pressure freezer (EM PACT2, Leica) followed by freeze substitution, infiltration, and embedding in HM20. UV polymerization was performed at –35 °C. Immunogold labelling was performed on HPF ultrathin sections using an anti-VSR antibody. Transgenic cells without heat shock treatment were used as corresponding controls. The preparation of EM samples was performed according to established protocols (Jiang *et al*., 2000; Tse *et al*., 2004; Wang *et al*., 2007; Gao *et al*., 2012). Transmission EM examination was done with a Hitachi H-7650 transmission electron microscope with a charge-coupled device camera (Hitachi High-Technologies) operating at 80 kV.

Results

GFP–ARA7(Q69L) induces the formation of enlarged ring-like structures that co-localize with the MVB marker, VSR2, in Arabidopsis *protoplasts*

To determine the subcellular localization of ARA7(Q69L) in *Arabidopsis* cells, GFP–ARA7 or GFP–ARA7(Q69L) was transiently expressed in *Arabidopsis* protoplasts derived from suspension-cultured PSBD cells. As shown in Fig. 1A, GFP-tagged WT ARA7 labelled punctate structures, whereas the constitutively active mutant GFP–ARA7(Q69L) localized to ring-like structures. To investigate the membrane nature of these ring-like structures, GFP–ARA7(Q69L) was transiently co-expressed with the mRFP-tagged MVB marker, VSR2, the TGN marker, SYP61, or the Golgi marker, ManI, in *Arabidopsis* protoplasts. As shown in Fig. 1B, only mRFP–VSR2 co-localized with GFP–ARA7(Q69L) on the membranes of enlarged spheres, which supports the MVB-derived nature of these ring-like structures. In contrast, there was no co-localization between GFP-labelled ring-like structures and either mRFP–SYP61 or mRFP–ManI (Fig. 1C, D), indicating that neither TGN nor Golgi membranes contribute to the enlarged spheres.

Generation and characterization of transgenic Arabidopsis *PSBD cell lines expressing GFP–ARA7(Q69L) under the control of a heat shock promoter*

To investigate the nature of these GFP–ARA7(Q69L)-induced ring-like structures further, transgenic *Arabidopsis* cell lines stably expressing GFP–ARA7(Q69L) under the control of a HSP were generated via *A. tumefaciens*-mediated transformation. To induce GFP–ARA7(Q69L) fusion protein expression, transgenic cells were subjected to a brief heat shock treatment at 37 °C for 1 h and then immediately incubated at 27 °C for an additional 1–8 h before analysis of the GFP signals. To confirm the involvement of GFP–ARA7(Q69L) in the formation of these ring-like structures, time-course experiments were performed by confocal imaging and western blot analysis. As shown in Fig. 2A, no GFP signal was detected by confocal microscopy before heat shock treatment. However, cytosolic GFP signals were detected in transgenic cells exposed to heat shock after a 2 h incubation. In addition, the number of GFP-positive ring-like structures increased significantly after 4 h, and most signals were visible at the tonoplast after 6 h. Consistent results were also obtained by western blot analysis with an anti-GFP antibody. A band corresponding to the GFP fusion protein was first detected 2 h after heat shock treatment (Fig. 2B). The anti-GFP antibody did not recognize epitopes in WT or transgenic cells without heat shock treatment. An anti-tubulin antibody was used as an internal control to ensure equal loading of proteins.

Taken together, these results demonstrate that expression of GFP–ARA7(Q69L) in transgenic cells is controlled by heat shock treatment, which induces the formation of GFP-labelled ring-like structures. It should be noted that a 4 h incubation was used for all subsequent experiments because the localization of GFP–ARA7(Q69L) to enlarged spheres was highest at this time point (as assessed by confocal microscopy).

Membrane fusion of GFP–ARA7(Q69L)-labelled organelles in transgenic cells

To study the events leading up to the formation of these ring-like structures, transgenic cells expressing GFP–ARA7(Q69L) were subjected to heat shock treatment followed by time-lapse collection of GFP signals by spinning disc confocal microscopy. GFP signals were visible as small but highly mobile punctate structures that fused to create larger ring-like structures. Multiple fusion events were observed, such as those between two enlarged ring-like structures (Fig. 3; Supplementary Video S1 available at *JXB* online), a punctate and a ring-like structure (Supplementary Fig. S1; Video S2), and two vacuole-like structures (Supplementary Fig. S2; Video S3). These results indicate that the larger ring-like structures are derived largely from the active fusion of smaller

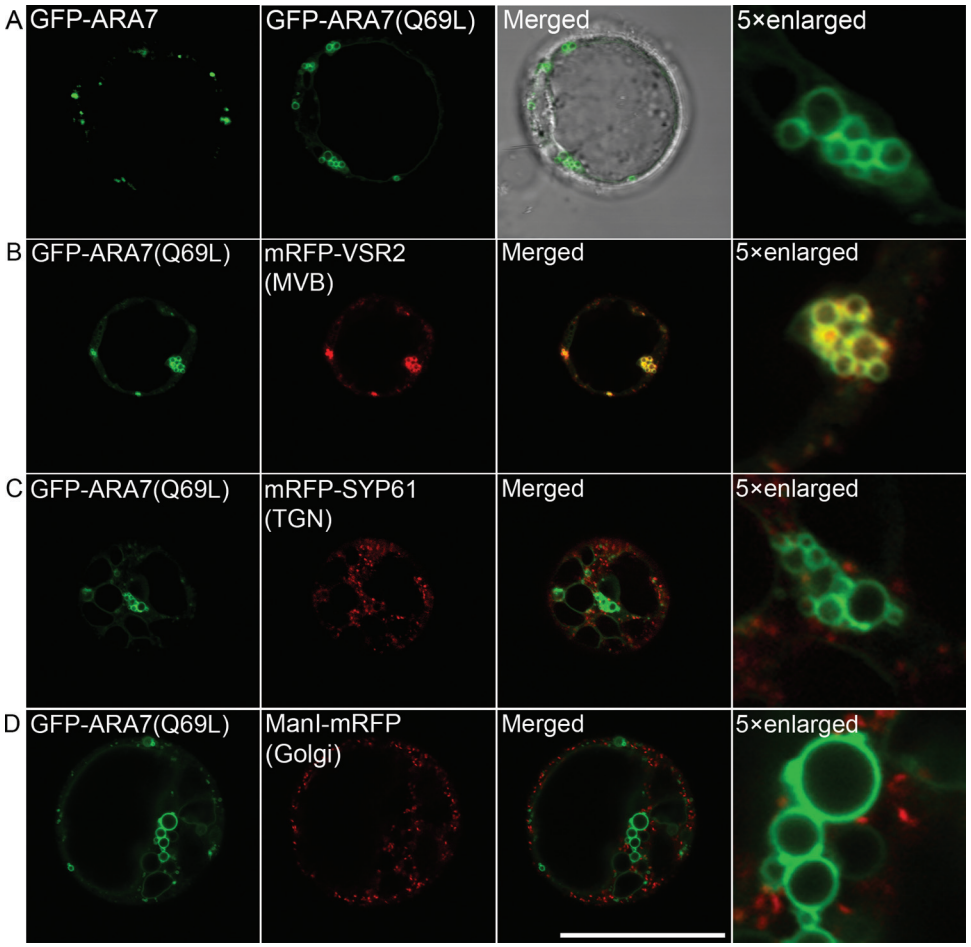

Fig. 1. GFP–ARA7(Q69L)-induced ring-like structures co-localize with an MVB marker, but not with TGN or Golgi markers, in *Arabidopsis* protoplasts. (A) The GFP fusion construct GFP–ARA7 or the GTP-bound mutant GFP–ARA7(Q69L) were transiently expressed in *Arabidopsis* protoplasts followed by confocal imaging. (B–D) GFP–ARA7(Q69L) was transiently co-expressed with the mRFP-tagged MVB marker, mRFP–VSR2, the TGN marker, mRFP–SYP61, or the Golgi marker, ManI–mRFP, in *Arabidopsis* protoplasts, followed by confocal imaging. Enlarged images of selected areas are also shown (A–D). Scale bar=50 μm.

GFP-positive structures and that GFP–ARA7(Q69L) is likely to accumulate on the tonoplast and to promote vacuole fusion.

GFP–ARA7(Q69L) co-localizes with the PVC/MVB marker, VSR, on enlarged MVBs but not with TGN and Golgi markers in transgenic Arabidopsis *cell lines*

To elucidate further the membrane source of these enlarged MVBs in transgenic *Arabidopsis* cell lines, immunofluorescence was performed using (i) anti-VSR (a MVB marker); (ii) anti-SYP61 (a TGN marker); (iii) anti-ManI (a *cis*-Golgi marker); and (iv) anti-VPPase (a tonoplast marker) antibodies. As shown in Fig. 4, VSR co-localized with the GFP signal on the limiting membrane of ring-like structures, but was distinct from SYP61 and ManI. In addition, VPPase co-localized with GFP–ARA7(Q69L) on ring-like structures. In WT or transgenic cells without heat shock treatment, the anti-VSR antibody labelled punctate PVC structures (Supplementary Fig. S3 at *JXB* online). These results indicate that heat shock treatment itself does not affect the distribution of VSRs or the morphology of MVBs, and that untreated (without heat shock) transgenic GFP–ARA7(Q69L) cells are physiologically similar to WT cells. Taken together, the immunofluorescence results obtained using the transgenic cell lines are identical to those obtained using *Arabidopsis* protoplasts.

To investigate further the localization of GFP–ARA7(Q69L), immunogold-EM experiments were performed. First, transgenic GFP–ARA7(Q69L) *Arabidopsis* cells were either subjected to [GFP–ARA7(Q69L)+] or not subjected to [GFP–ARA7(Q69L)–] a brief heat shock treatment, which was then followed by HPF, ultrathin sectioning, and immunogold labelling using an anti-VSR antibody. As shown in Fig. 5, the VSR antibody specifically labelled MVBs with a diameter of ~300 nm in transgenic cells without heat shock treatment. On the other hand, the limiting membrane of clustered and enlarged MVBs with a diameter >500 nm in transgenic cells was immunoreactive for VSR upon heat shock treatment. To conclude, the immunogold-EM experiments confirmed that the ARA7(Q69L)-induced ring-like structures in transgenic cells were MVBs.

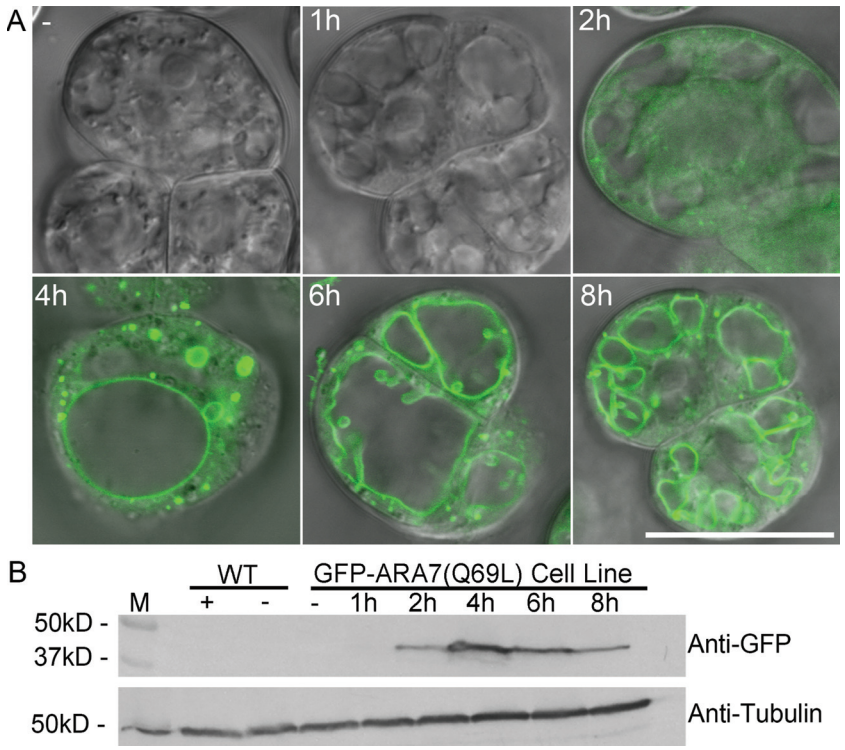

Fig. 2. Analysis of GFP–ARA7(Q69L) expression and localization in transgenic *Arabidopsis* cells. (A, B) Transgenic GFP–ARA7(Q69L) cells were subjected to heat shock treatment for different durations as indicated (+), followed by either confocal microscopy or western blot analysis using anti-GFP or anti-tubulin antibodies. Transgenic *Arabidopsis* cells without heat shock treatment (–) were used as the corresponding control. Scale bar=25 μm. (This figure is available in colour at *JXB* online.)

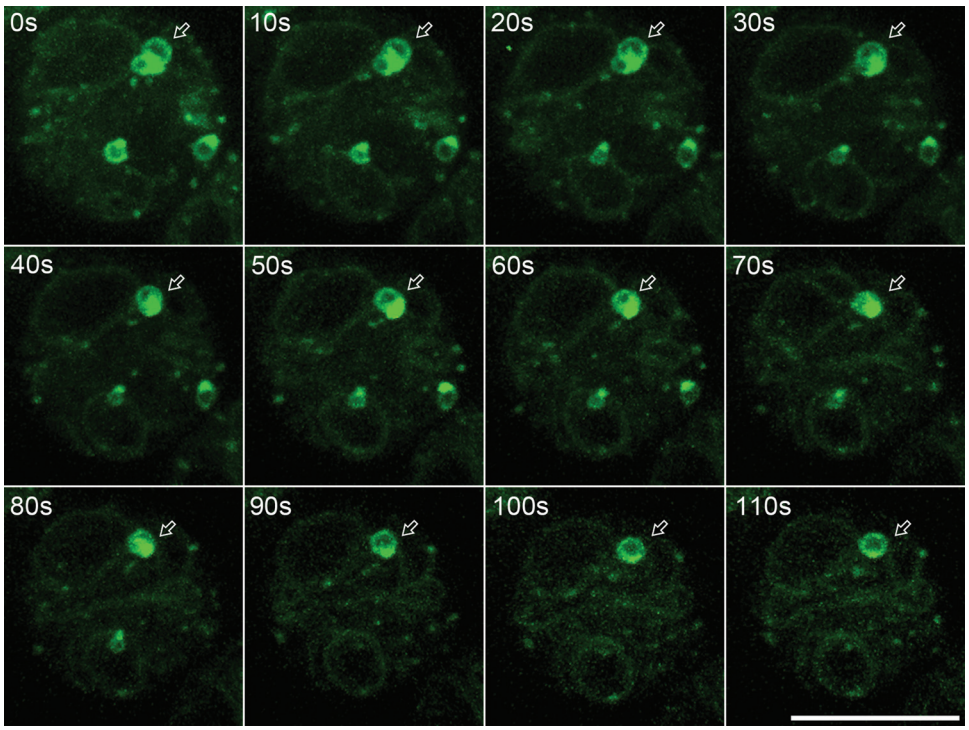

Fig. 3. Membrane fusion of two enlarged GFP–ARA7(Q69L)-labelled ring-like structures in transgenic Arabidopsis cells. Time-lapse images of transgenic cells expressing GFP–ARA7(Q29L) were collected by confocal microscopy. Arrows point to the fusion of two enlarged ring-like structures. Scale bar=10 μm.

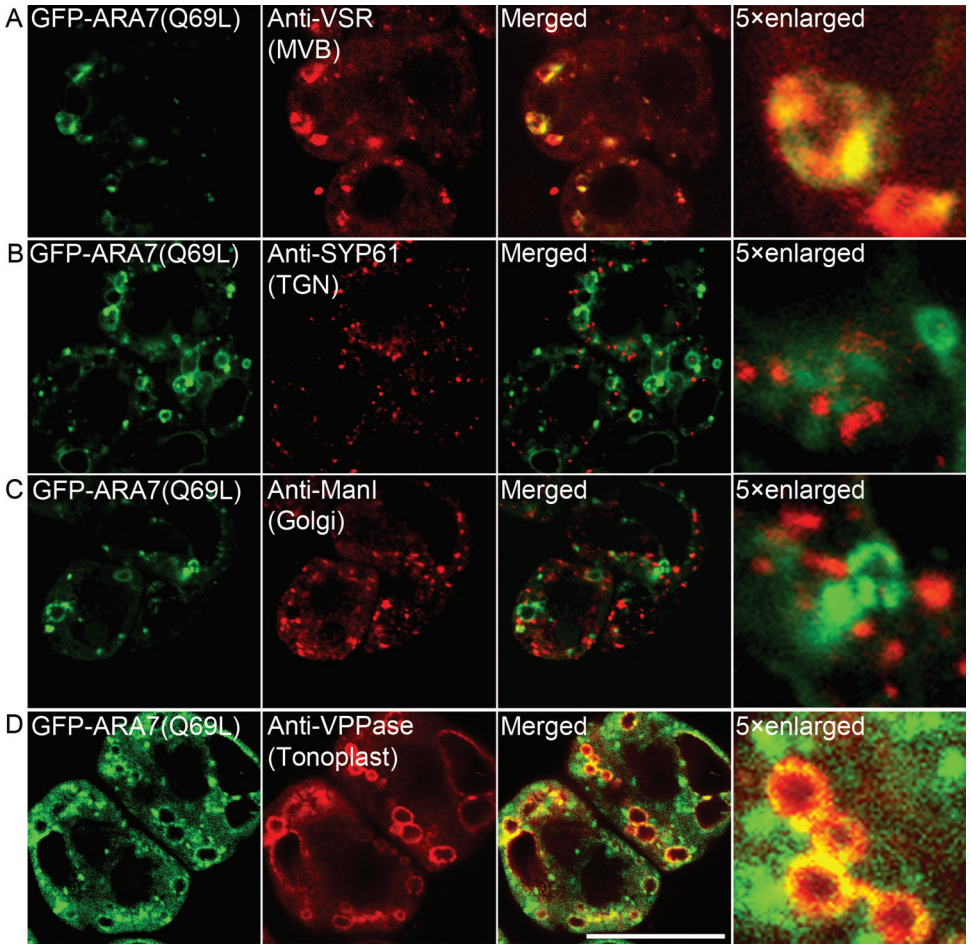

Fig. 4. GFP–ARA7(Q69L) co-localizes with VSR and VPPase on ring-like structures, but not with TGN or Golgi markers in transgenic *Arabidopsis* cells. Transgenic GFP–ARA7(Q69L) cells were subjected to heat shock treatment, followed by chemical fixation, immunostaining with different antibodies (i.e. anti-VSR, anti-SYP61, anti-ManI, or anti-VPPase), and confocal imaging. Enlarged images of selected areas are also shown. Scale bar=25 μm.

Ultrastructural analysis of enlarged MVBs induced by GFP–ARA7(Q69L) expression

To gain additional insight into the formation of ARA7(Q69L)-induced enlarged MVBs, ultrastructural analysis was performed using transmission electron microscopy (TEM).

As shown in Supplementary Fig. S4 at *JXB* online, transgenic cells without heat shock treatment contained one large central vacuole. However, upon heat shock treatment, many enlarged MVBs, or small vacuoles with different diameters, were observed in transgenic cells. In both chemically fixed (Fig. 6A) and HPF samples (Fig. 6B), the cells without GFP–ARA7(Q69L) expression contained normal MVBs with a diameter ~200–500 nm. In contrast, the morphology and size of the MVBs in GFP–ARA7(Q69L)-expressing cells were very different. As shown in Fig. 6, in the cells treated with heat shock, lots of MVBs were usually found to accumulate as clusters and become fused. Furthermore, many enlarged MVBs, ranging from 500 nm to 1 μm in diameter with typical internal vesicles, were readily observed in the GFP–ARA7(Q69L)-expressing cells (Fig. 7). In addition, examples of extremely enlarged MVBs, ~1.5 μm in diameter, but containing very few internal vesicles, were also observed (Fig. 8). Statistical analyses showed the average diameter of enlarged MVBs in GFP–ARA7(Q69L)+ cells to be approximately three times greater than that in GFP–ARA7(Q69L)– cells, while the number of internal vesicles was at least 10 times less than those in untreated cells (Table 1).

In conclusion, both live cell imaging and ultrastructural analyses provided substantial evidence demonstrating that GFP–ARA7(Q69L)-induced ring-like structures were derived from an overabundance of homotypic fusion of MVBs.

ARA7(Q69L) can be used as a useful tool to distinguish the protein locations on MVBs

Since ARA7(Q69L) expression induced the formation of enlarged MVBs, proteins either on the membrane or within the lumen of the enlarged MVBs could be easily distinguished under light microscopy. Thus, when mRFP-tagged ARA7(Q69L) was used in the co-expression experiments, the subcellular localization and fate of GFP-tagged proteins

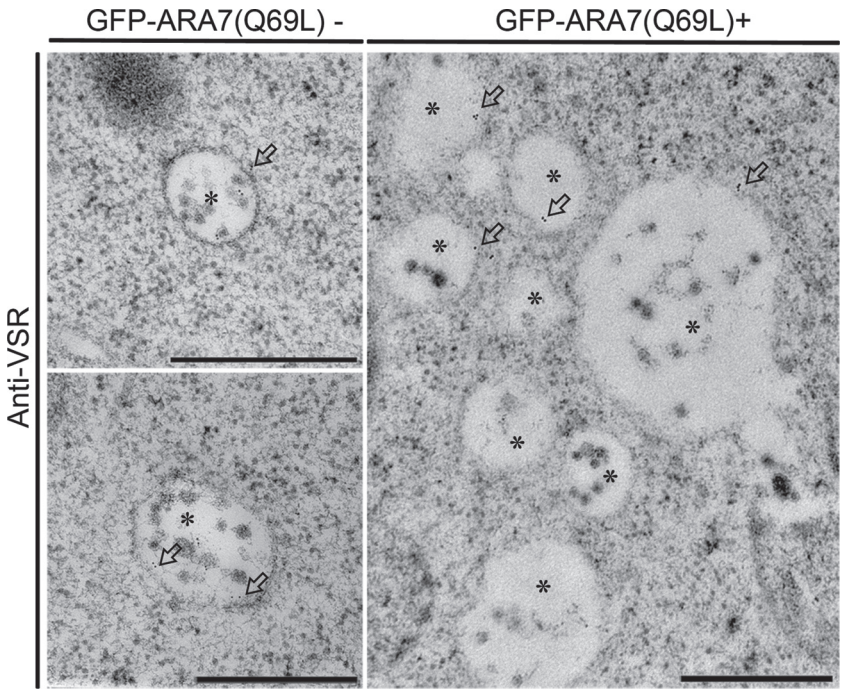

Fig. 5. Immunogold-EM analysis confirms VSR labelling of enlarged ring-like structures (i.e. enlarged MVBs). Transgenic GFP–ARA7(Q69L) *Arabidopsis* cells were subjected to heat shock treatment (+) followed by HPF and immunolabelling with an anti-VSR antibody. Transgenic *Arabidopsis* cells without heat shock treatment (–) were used as the corresponding control. VSR-labelled normal MVBs (asterisks) in untreated cells and VSR-labelled enlarged MVBs (asterisks) in treated cells are shown. Arrows point to immunoreactive gold particles (6 nm). Scale bar=500 nm.

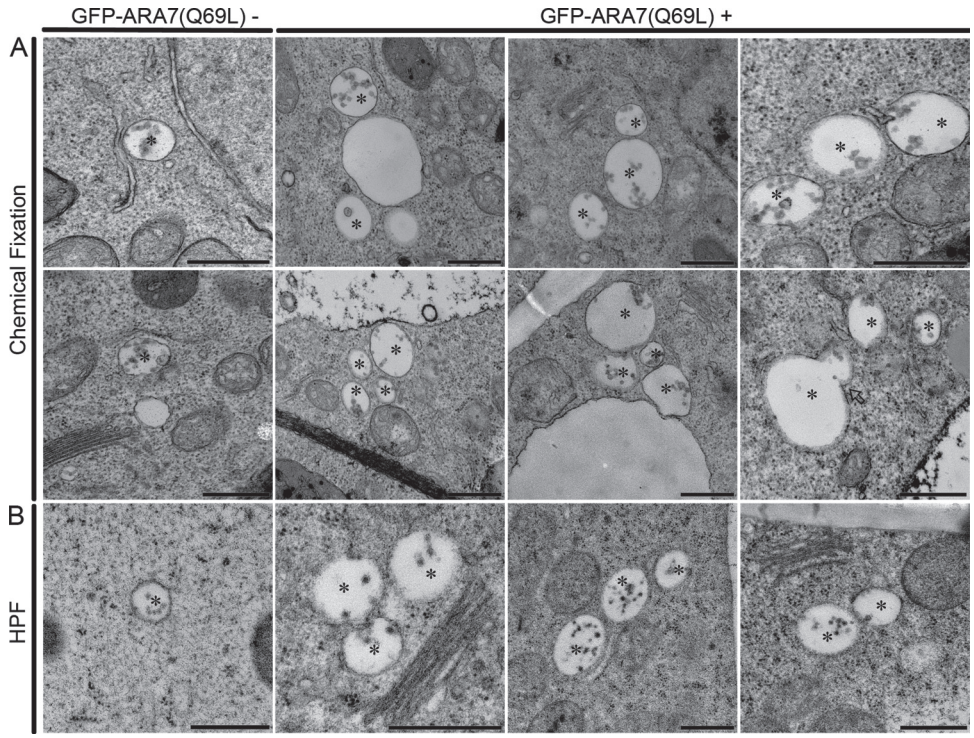

Fig. 6. TEM analysis of clusters of MVBs in transgenic *Arabidopsis* cells expressing GFP–ARA7(Q69L). Transgenic GFP–ARA7(Q69L) *Arabidopsis* cells were subjected to heat shock treatment (+) followed by chemical fixation (A) or HPF (B) and subsequent TEM analysis. Transgenic *Arabidopsis* cells without heat shock treatment (–) were used as the corresponding control. Clustered MVBs (asterisks) are shown. Arrow points to fusion between two MVBs. Scale bar=500 nm.

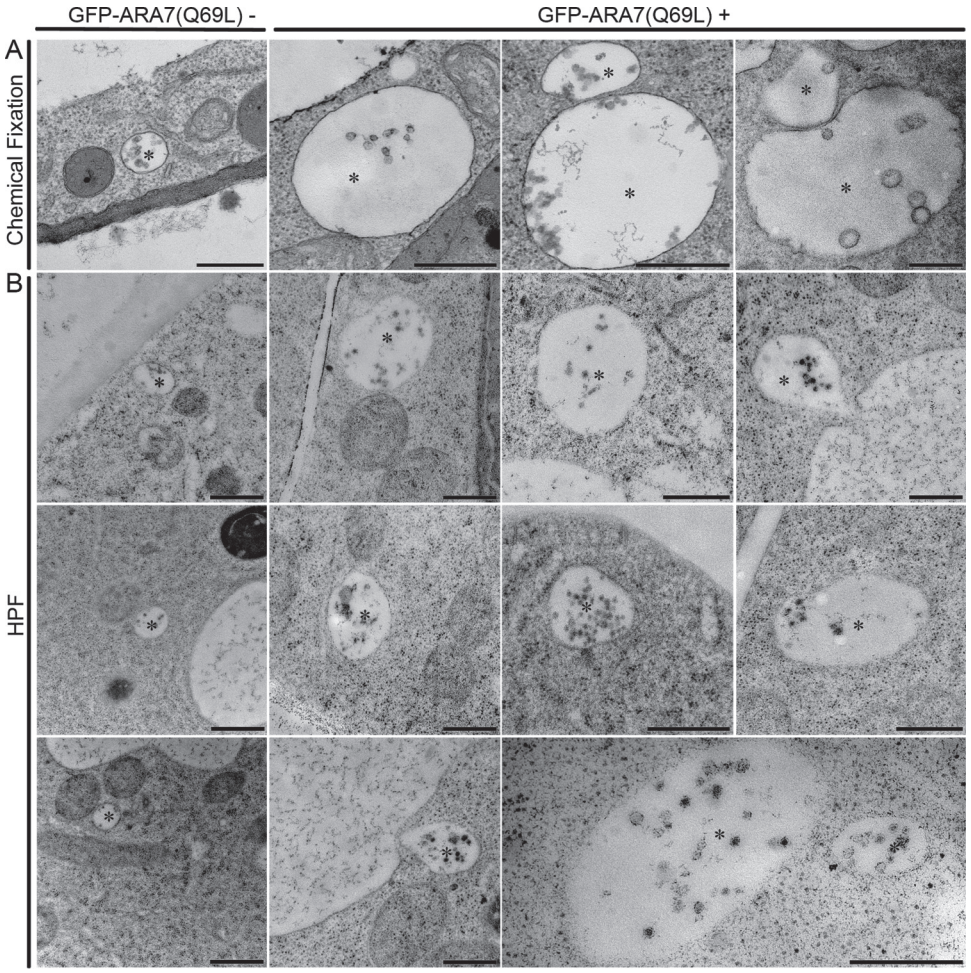

Fig. 7. Ultrastructure of enlarged MVBs in transgenic *Arabidopsis* cells expressing GFP–ARA7(Q69L). Transgenic GFP–ARA7(Q69L) *Arabidopsis* cells were subjected to heat shock treatment (+) followed by chemical fixation (A) or HPF (B) and subsequent TEM analysis. Transgenic *Arabidopsis* cells without heat shock treatment (–) were used as the corresponding control. Enlarged MVBs (asterisks) ranging from 500 nm to 1 μm in diameter with typical internal vesicles are shown. Scale bar=500 nm.

in the MVBs could be determined, thereby defining MVB-mediated protein recycling or degradation in plant cells.

Indeed, as proof-of-principle, mRFP–ARA7(Q69L) was transiently co-expressed with different GFP-tagged marker proteins in *Arabidopsis* protoplasts (Fig. 9). Aleurain–GFP is a soluble vacuolar cargo reporter (Miao *et al*., 2008). EMP12–GFP (endomembrane protein 12 tagged with GFP at the C-terminus) is a membrane protein destined for MVB-mediated vacuolar degradation (Gao *et al*., 2012), whereas VAMP727 (vesicle-associated membrane protein 727) and VTI11 (vacuolar protein sorting ten interacting 11) are components of the SNARE complex, which mediate fusion between the PVC and the vacuolar membrane (Ebine *et al*., 2008). Finally, VIT1 (vacuolar iron transporter1) was used as a marker of the tonoplast (Kim *et al*., 2006). As shown in Fig. 9, aleurain–GFP and EMP12–GFP were trapped within the lumen of enlarged MVBs for further vacuolar targeting and degradation (Fig. 9A, B), while VAMP727, VTI11, and VIT1 were localized to the limiting membrane of enlarged MVBs, but not internalized into the lumen of MVBs (Fig. 9C–E). Thus, enlarged MVBs allow not only the study of MVB-mediated protein trafficking, but also determination of the fate of a given protein based on its distinct localization on the limiting membrane or within the lumen of enlarged MVBs.

Since wortmannin induces PVC/MVB enlargement in plant cells (Tse *et al*., 2004; Wang *et al*., 2009), its effects were compared with those of ARA7(Q69L) expression on MVBs. As described above, mRFP–ARA7 was transiently co-expressed with the same protein markers (i.e. aleurain–GFP, EMP12–GFP, VAMP727–GFP, VTI11–GFP, and VIT1–GFP) into *Arabidopsis* protoplasts followed by wortmannin treatment and confocal imaging. As shown in Supplementary Fig. S5 at *JXB* online, aleurain–GFP and EMP12–GFP were trapped within the lumens of enlarged MVBs, similar to the effects of ARA7(Q69L) (Supplementary Fig. S5A, B), while VAMP727, VTI11, and VIT1 remained on the limiting membranes (Supplementary Fig. S5C–E). Taken together, ARA7(Q69L) can mimic the effects of wortmannin to induce formation of enlarged MVBs, which can then be used to distinguish the subcellular distribution and fate of different proteins on MVBs in plant cells.

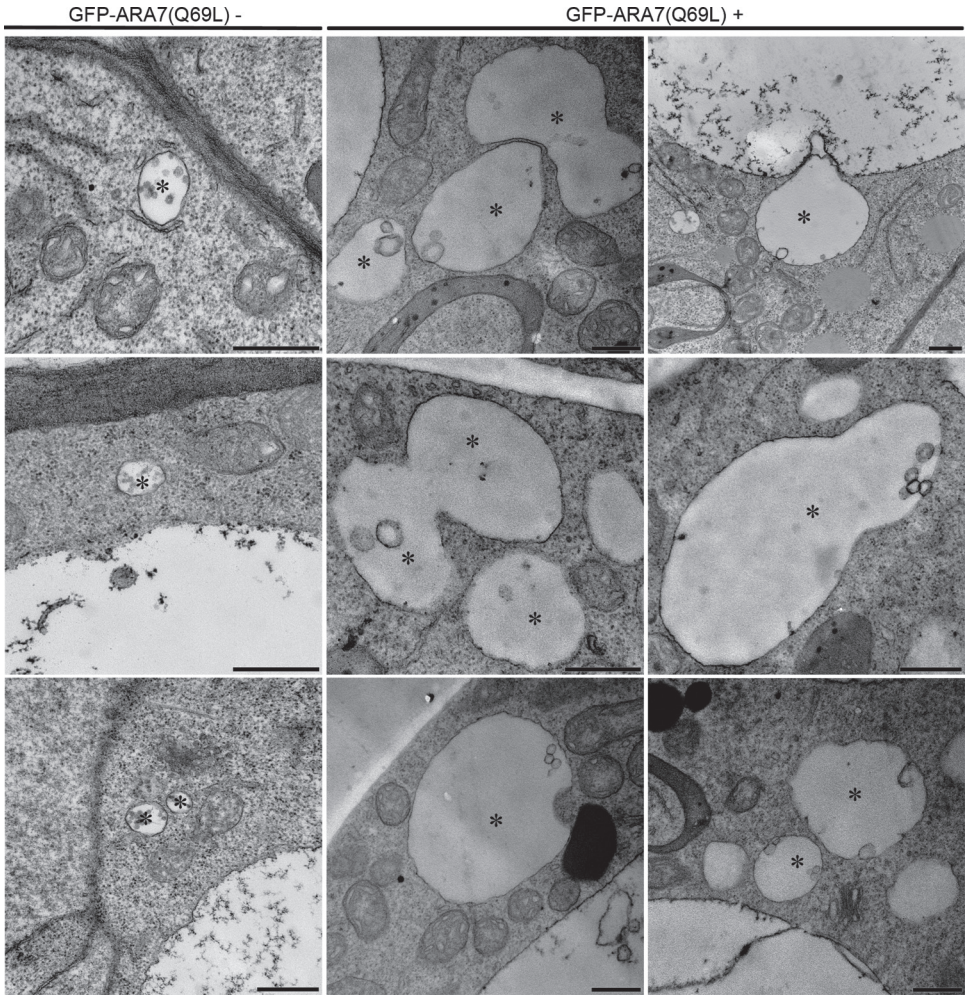

Fig. 8. Ultrastructure of extremely enlarged structures with few internal vesicles in transgenic *Arabidopsis* cells following GFP–ARA7(Q69L) expression. Transgenic GFP–ARA7(Q69L) *Arabidopsis* cells were subjected to heat shock treatment (+) followed by chemical fixation and subsequent TEM analysis. Transgenic *Arabidopsis* cells without heat shock treatment (–) were used as the corresponding control. Enlarged MVBs (asterisks) with a diameter >1.5 μm with few internal vesicles are shown. Scale bar=500 nm.

Discussion

The small GTPase Rab5 localizes to early endosomes and regulates endocytic trafficking in mammalian cells (Bucci *et al.*, 1992). The GTPase-deficient Rab5 mutant, Rab5(Q79L), stimulates endosomal fusion, causing the formation of enlarged endosomes in mammalian cells (Stenmark *et al.*, 1994). Moreover, immunofluorescence and immuno-EM labelling analysis reveal that Rab5(Q79L)-induced enlarged endosomes contain both early and late endosomal marker proteins, which thus suggests that overexpression of Rab5(Q79L) not only induces formation of enlarged early endosomes but also causes enlargement of later endocytic endosomes (Hirota *et al.*, 2007; Wegner *et al.*, 2010).

Similar to the effects of Rab5(Q79L) in mammalian cells, expression of GTPase-defective mutants, ARA7(Q69L), RHA1(Q69L), and ARA6(Q93L), also induces the formation of ring-like structures in plant cells (Ueda *et al.*, 2001; Kotzer

Table 1. Effects of GFP–ARA7(Q69L) expression on MVB size and internal vesicle number.

Cell line	Average diameter of MVBs (nm), mean ±SD	Total no. of MVBs	Total no. of internal vesicles	Average no. of vesicles per MVB	Average no. of internal vesicles per MVB (expressed per μm^2)
GFP–ARA7(Q69L)+	1046.58 ± 529.7*	25	289	11.6	10.8**
GFP–ARA7(Q69L)–	302.1 ± 84.4*	20	238	11.9	125**

Significant differences between heat shock-treated (+) and untreated (–) groups were analysed using a two-tailed *t*-test (*$P < 0.001$,**$P < 0.001$). Data were collected and analysed from three independent experiments.

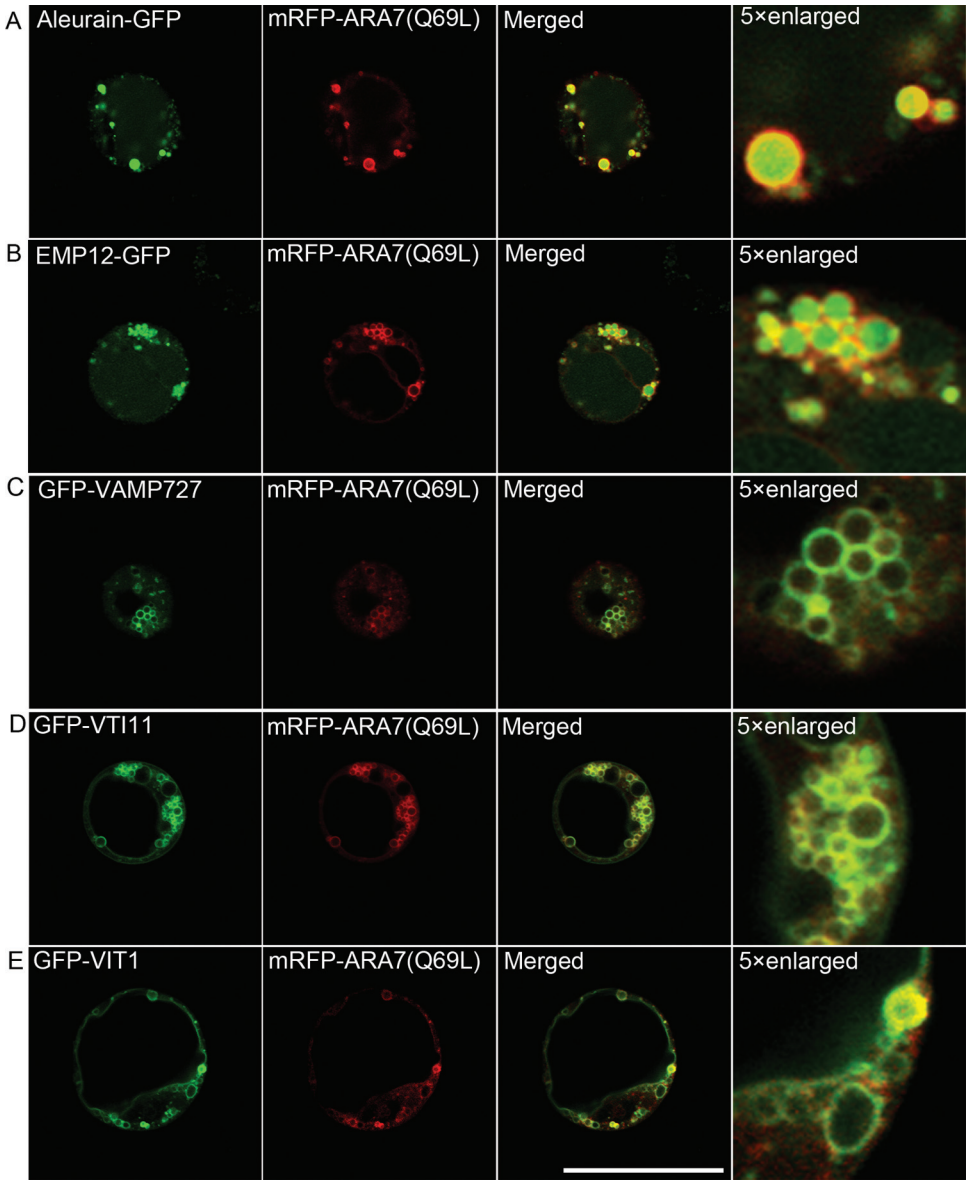

Fig. 9. Different distribution of degradative and functional proteins on ARA7(Q69L)-induced enlarged MVBs. mRFP–ARA7(Q69L) was transiently co-expressed with aleurain–GFP (A), EMP12–GFP (B), VAMP727–GFP (C), VTI11–GFP (D), or VIT1–GFP (E) in *Arabidopsis* protoplasts, followed by confocal imaging. Note that the degradative cargo proteins were trapped within the lumen of enlarged MVBs induced by mRFP–ARA7(Q69L) overexpression (A, B), whereas, the PVC/tonoplast-localized functional proteins co-localized with mRFP–ARA7(Q69L) on the limiting membrane of enlarged MVBs. Enlarged images of selected areas are also shown. Scale bar=50 μm.

et al., 2004; Lee *et al*., 2004; Cai *et al*., 2011; Ebine *et al*., 2011). In 2004, Kotzer *et al*. suggested that ARA7(Q69L)-induced spheres could possibly be enlarged PVCs because they co-localized with a PVC marker protein and trapped aleurain within the lumen of tobacco leaf epidermal cells (Kotzer *et al*., 2004). However, ARA7(Q69L)-induced ring-like structures have never been characterized at the ultrastructural level in plant cells. Therefore, the goal of the present study was to characterize the ultrastructure, membrane origins, and dynamics of ARA7(Q69L)-induced ring-like structures using transgenic *Arabidopsis* cell lines expressing inducible GFP–ARA7(Q69L). It is demonstrated that these ARA7(Q69L)-induced ring-like structures mainly result from the homotypic fusion of MVBs, with no involvement of early endosomes, the TGN, or the Golgi apparatus.

First, GFP–ARA7(Q69L) transgenic *Arabidopsis* cell lines were characterized by confocal microscopy and western blot analyses. Interestingly, GFP signals were first detected in the cytosol, but then concentrated as punctate dots localizing to enlarged ring-like structures and, finally, accumulated on the tonoplast. The accumulation of GFP signals on tonoplasts could be explained by reduced GTP hydrolysis. The slow recycling of ARA7(Q69L) may result in its transport to the vacuolar membrane by a default pathway, which is also consistent with previous findings (Kotzer *et al*., 2004; Lee *et al*., 2004). Subsequent immunofluorescence analysis showed

that ARA7(Q69L)-induced ring-like structures co-localized with the MVB marker, VSR, on the limiting membrane, but it did not co-localize with the TGN marker, SYP61, or the Golgi marker, ManI. In addition, immunogold-EM analysis confirmed VSR labelling on enlarged MVBs. These results demonstrate the MVB-derived membrane nature of ARA7(Q69L)-enlarged ring-like structures. After having identified the nature of these ring-like structures, the ultrastructure of enlarged MVBs was also examined. TEM analysis showed that GFP–ARA7(Q69L)-induced enlarged MVBs were derived largely from the homotypic fusion of PVCs.

Based on TEM analysis, the number of internal vesicles in ARA7(Q69L)-expressing cells was reduced considerably compared with that in control cells, especially in enlarged MVBs having a diameter >1.5 μm. One reason for this may be that internal vesicles fused with the limiting MVB membrane. However, the digestion of internal vesicles resulting from the acidification of enlarged MVBs seems to be a more plausible explanation. Because of the fusion of MVBs, protons pumps targeting the vacuole (e.g. vacuolar-type H^+-translocating ATPase and VPPase) are likely to accumulate on the membrane of rapidly enlarged MVBs and acidify the MVB lumens. The intense labelling of the limiting membrane of enlarged MVBs by an anti-VPPase antibody was taken as an indication that the lumen of enlarged MVBs was becoming increasingly acidic. The acidification of the enlarged MVBs was indicated by the neutral red staining experiments as shown in Supplementary Fig. S6 at *JXB* online. Neutral red is a pH indicator, which changes its colour from yellow to red when the pH is below 6.8. The strong red colour of neutral red in the lumen of the ARA7(Q69L)-induced sphere structure indicated the acidic nature of these enlarged MVBs. Thus, the enlarged MVBs have an acidic lumen.

Since it has been shown that overexpression of the constitutively active rab5 mutant, GFP–ARA7(Q69L), but not the WT version, GFP–ARA7, induces the enlargement of MVBs to form large ring-like structures, which can also be induced by expression of the tag-free ARA7(Q69L) mutant protein (Supplementary Fig. S7 at *JXB* online), ARA7(Q69L) can thus be used as a convenient and reliable tool to study the subcellular distributions of different proteins on MVBs. Indeed, the present results demonstrated that ARA7(Q69L)-enlarged MVBs trapped degradative cargo (i.e. aleurain–GFP and EMP12–GFP) within the lumen and that the MVB- and tonoplast-localized functional proteins (i.e. VAMP727, VTI11, and VIT1) co-localized with mRFP–ARA7(Q69L) on the limiting membrane. Previous research has shown that wortmannin can induce the formation of enlarged/vacuolated MVBs in plant cells (Tse *et al*., 2004; Wang *et al*., 2009; Miao *et al*, 2011). In the present study, the effects of wortmannin were compared with those of ARA7(Q69L). Similarly, proteins targeted for vacuolar degradation were trapped within the lumen, while proteins functioning on MVB or vacuolar membranes were localized to the limiting membrane of enlarged MVBs. These results illustrate that wortmannin elicits similar effects with ARA7(Q69L) and induces MVB enlargement in plant cells, which is similar to wortmannin mimicking the Rab5(Q79L) effect in mammalian cells (Chen and Wang, 2001). In mammalian cells, wortmannin treatment can stimulate Rab5 activity by blocking the interaction between Rab5 and p120 Ras GAP and thus mimic the effect of Rab5(Q79L) on intracellular trafficking (Chen and Wang, 2001). In plant cells, expression of ARA7(Q69L) also mimics the effect of wortmannin in inducing the enlargement of MVBs. However, multiple mechanisms are probably responsible for providing the membranes needed for the rapid wortmannin-induced enlargement of PVCs in plant cells, including homotypic fusion of MVBs, fusion between TGN and MVBs, and fusion between MVB internal vesicles and the outer membrane (Tse *et al*., 2004; Miao *et al*., 2006, 2008; Wang *et al*., 2009, 2013). In addition to the effects on the enlargement of MVBs, wortmannin also has a strong inhibitory effect even on the early endocyte since it prevents the uptake of the fluorescent dye FM4-64 at the plasma membrane (Emans *et al*., 2002). The exact molecular targets and inhibitory mechanisms of wortmannin in plant cells remain elusive. Compared with wortmannin, ARA7(Q69L) is a more specific tool to induce homotypic fusion of MVBs, and ARA7(Q69L) does not induce the fusion between the TGN and MVBs, and does not exert inhibitory effects on the endocytic pathway. In addition, it was noticed that the wortmannin treatment hardly had an additive effect on ARA7(Q69L)-induced phenotypes (Supplementary Fig. S8 at *JXB* online), thus ARA7(Q69L) has a much stronger effect than wortmannin treatment on the enlargement of MVBs. Since the sizes of ARA7(Q69L)-induced enlarged MVBs are usually larger than those caused by wortmannin treatment, it will be much easier to distinguish the relative distribution of proteins on the limiting membrane or the lumen of MVBs using the expression of ARA7(Q69L).

In summary, it has been shown that GFP–ARA7(Q69L) expression induced the formation of spherical structures and that they originated largely from the homotypic fusion of MVBs. It was also shown that ARA7(Q69L) expression is a useful model that can be used to study the biology of different proteins on MVBs.

Supplementary data

Supplementary data are available at *JXB* online

Figure S1. Dynamics of membrane fusion between two GFP–ARA7(Q69L)-labelled organelles in transgenic cells.

Figure S2. Dynamics of membrane fusion and internalization between two enlarged GFP–ARA7(Q69L)-labelled organelles in transgenic cells.

Figure S3. GFP–ARA7(Q69L) co-localized with anti-VSR on enlarged MVBs.

Figure S4. Structural TEM analysis of overall cell morphology of transgenic *Arabidopsis* cells.

Figure S5. Wortmannin-induced enlarged MVBs trap the degradative cargo proteins within their lumen, but were labelled by the PVC/tonoplast-localized functional proteins on the limiting membrane.

Figure S6. The enlarged MVBs induced by GFP–ARA7(Q69L) have an acidic lumen.

Figure S7. Tag-free ARA7(Q69L) induces formation of enlarged ring-like structures (MVBs) labelled by GFP–VAMP727 and GFP–VTI11 at the limiting membrane.

Figure S8. Wortmannin treatment does not have an additive effect on the GFP–ARA7(Q69L)-induced phenotype (enlarged MVBs).

Video S1. Video showing membrane fusion of two enlarged GFP–ARA7(Q69L)-labelled ring-like structures in transgenic *Arabidopsis* cells.

Video S2. Video showing membrane fusion of two GFP–ARA7(Q69L)-labelled organelles in transgenic cells.

Video S3. Video showing membrane fusion and internalization of two enlarged GFP–ARA7(Q69L)-labelled organelles in transgenic cells.

Acknowledgements

We thank Prof Karin Schumacher (Heidelberg University, Germany) for providing us the pHGT1 vector containing the heat shock promoter (hsp18.2). This work was supported by grants from the Research Grants Council of Hong Kong (CUHK466309, CUHK466610, CUHK466011, CUHK465112, CUHK2/CRF/11G), NSFC/RGC (N_CUHK406/12), and CUHK Schemes to LJ.

References

Bucci C, Parton RG, Mather IH, Stunnenberg H, Simons K, Hoflack B, Zerial M. 1992. The small Gtpase Rab5 functions as a regulatory factor in the early endocytic pathway. *Cell* **70,** 715–728.

Cai Y, Jia T, Lam SK, Ding Y, Gao C, San MW, Pimpl P, Jiang L. 2011. Multiple cytosolic and transmembrane determinants are required for the trafficking of SCAMP1 via an ER–Golgi–TGN–PM pathway. *The Plant Journal* **65,** 882–896.

Cai Y, Zhuang X, Wang J, Wang H, Lam SK, Gao C, Wang X, Jiang L. 2012. Vacuolar degradation of two integral plasma membrane proteins, AtLRR84A and OsSCAMP1, is cargo ubiquitination-independent and prevacuolar compartment-mediated in plant cells. *Traffic* **13,** 1023–1040.

Chen PY, Wang CK, Soong SC, To KY. 2003. Complete sequence of the binary vector pBI121 and its application in cloning T-DNA insertion from transgenic plants. *Molecular Breeding* **11,** 287–293.

Chen XM, Wang ZX. 2001. Regulation of epidermal growth factor receptor endocytosis by wortmannin through activation of Rab5 rather than inhibition of phosphatidylinositol 3-kinase. *EMBO Reports* **2,** 842–849.

Ding Y, Wang J, Wang J, Stierhof Y-D, Robinson DG, Jiang L. 2012. Unconventional protein secretion. *Trends in Plant Science* **17,** 606–615.

Ebine K, Fujimoto M, Okatani Y, *et al.* 2011. A membrane trafficking pathway regulated by the plant-specific RAB GTPase ARA6. *Nature Cell Biology* **13,** 853–859.

Ebine K, Okatani Y, Uemura T, *et al.* 2008. A SNARE complex unique to seed plants is required for protein storage vacuole biogenesis and seed development of Arabidopsis thaliana. *The Plant Cell* **20,** 3006–3021.

Emans N, Zimmermann S, Fischer R. 2002. Uptake of a fluorescent marker in plant cells is sensitive to brefeldin A and wortmannin. *The Plant Cell* **14,** 71–86.

Foresti O, Denecke J. 2008. Intermediate organelles of the plant secretory pathway: identity and function. *Traffic* **9,** 1599–1612.

Gao C, Yu CK, Qu S, San MW, Li KY, Lo SW, Jiang L. 2012. The Golgi-localized Arabidopsis endomembrane protein12 contains both endoplasmic reticulum export and Golgi retention signals at its C terminus. *The Plant Cell* **24,** 2086–2104.

Geldner N, Anders N, Wolters H, Keicher J, Kornberger W, Muller P, Delbarre A, Ueda T, Nakano A, Jurgens G. 2003. The Arabidopsis GNOM ARF-GEF mediates endosomal recycling, auxin transport, and auxin-dependent plant growth. *Cell* **112,** 219–230.

Haas TJ, Sliwinski MK, Martinez DE, Preuss M, Ebine K, Ueda T, Nielsen E, Odorizzi G, Otegui MS. 2007. The Arabidopsis AAA ATPase SKD1 is involved in multivesicular endosome function and interacts with its positive regulator LYST-INTERACTING PROTEIN5. *The Plant Cell* **19,** 1295–1312.

Hirota Y, Kuronita T, Fujita H, Tanaka Y. 2007. A role for Rab5 activity in the biogenesis of endosomal and lysosomal compartments. *Biochemical and Biophysical Research Communications* **364,** 40–47.

Jiang L, Phillips TE, Hamm CA, Drozdowicz YM, Rea PA, Maeshima M, Rogers SW, Rogers JC. 2001. The protein storage vacuole: a unique compound organelle. *Journal of Cell Biology* **155,** 991–1002.

Jiang L, Phillips TE, Rogers SW, Rogers JC. 2000. Biogenesis of the protein storage vacuole crystalloid. *Journal of Cell Biology* **150,** 755–770.

Jiang L, Rogers JC. 1998. Integral membrane protein sorting to vacuoles in plant cells: evidence for two pathways. *Journal of Cell Biology* **143,** 1183–1199.

Kim SA, Punshon T, Lanzirotti A, Li L, Alonso JM, Ecker JR, Kaplan J, Guerinot ML. 2006. Localization of iron in Arabidopsis seed requires the vacuolar membrane transporter VIT1. *Science* **314,** 1295–1298.

Kotzer AM, Brandizzi F, Neumann U, Paris N, Moore I, Hawes C. 2004. AtRabF2b (Ara7) acts on the vacuolar trafficking pathway in tobacco leaf epidermal cells. *Journal of Cell Science* **117,** 6377–6389.

Lam SK, Cai Y, Tse YC, Wang J, Law AH, Pimpl P, Chan HY, Xia J, Jiang L. 2009. BFA-induced compartments from the Golgi apparatus and trans-Golgi network/early endosome are distinct in plant cells. *The Plant Journal* **60,** 865–881.

Lam SK, Siu CL, Hillmer S, Jang S, An G, Robinson DG, Jiang L. 2007. Rice SCAMP1 defines clathrin-coated, trans-Golgi-located tubular–vesicular structures as an early endosome in tobacco BY-2 cells. *The Plant Cell* **19,** 296–319.

Lee GJ, Sohn EJ, Lee MH, Hwang I. 2004. The Arabidopsis rab5 homologs rha1 and ara7 localize to the prevacuolar compartment. *Plant and Cell Physiology* **45,** 1211–1220.

Li YB, Rogers SW, Tse YC, Lo SW, Sun SS, Jauh GY, Jiang L. 2002. BP-80 and homologs are concentrated on post-Golgi, probable lytic prevacuolar compartments. *Plant and Cell Physiology* **43,** 726–742.

Miao Y, Jiang L. 2007. Transient expression of fluorescent fusion proteins in protoplasts of suspension cultured cells. *Nature Protocols* **2,** 2348–2353.

Miao Y, Li HY, Shen J, Wang J, Jiang L. 2011. QUASIMODO 3 (QUA3) is a putative homogalacturonan methyltransferase regulating cell wall biosynthesis in Arabidopsis suspension-cultured cells. *Journal of Experimental Botany* **62,** 5063–5078.

Miao Y, Li KY, Li HY, Yao X, Jiang L. 2008. The vacuolar transport of aleurain–GFP and 2S albumin–GFP fusions is mediated by the same pre-vacuolar compartments in tobacco BY-2 and Arabidopsis suspension cultured cells. *The Plant Journal* **56,** 824–839.

Miao Y, Yan PK, Kim H, Hwang I, Jiang L. 2006. Localization of green fluorescent protein fusions with the seven Arabidopsis vacuolar sorting receptors to prevacuolar compartments in tobacco BY-2 cells. *Plant Physiology* **142,** 945–962.

Paris N, Stanley CM, Jones RL, Rogers JC. 1996. Plant cells contain two functionally distinct vacuolar compartments. *Cell* **85,** 563–572.

Ritzenthaler C, Nebenfuhr A, Movafeghi A, Stussi-Garaud C, Behnia L, Pimpl P, Staehelin LA, Robinson DG. 2002. Reevaluation of the effects of brefeldin A on plant cells using tobacco bright yellow 2 cells expressing Golgi-targeted green fluorescent protein and COPI antisera. *The Plant Cell* **14,** 237–261.

Sanderfoot AA, Kovaleva V, Bassham DC, Raikhel NV. 2001. Interactions between syntaxins identify at least five SNARE complexes within the Golgi/prevacuolar system of the Arabidopsis cell. *Molecular Biology of the Cell* **12,** 3733–3743.

Scheuring D, Viotti C, Kruger F, *et al.* 2011. Multivesicular bodies mature from the trans-Golgi network/early endosome in Arabidopsis. *The Plant Cell* **23,** 3463–3481.

Segev N. 2011. GTPases in intracellular trafficking: an overview. *Seminars in Cell and Developmental Biology* **22,** 1–2.

Shen Y, Wang J, Ding Y, Lo SW, Gouzerh G, Neuhaus JM, Jiang L. 2011. The rice RMR1 associates with a distinct prevacuolar compartment for the protein storage vacuole pathway. *Molecular Plant* **4,** 854–868.

Singer-Kruger B, Stenmark H, Zerial M. 1995. Yeast Ypt51p and mammalian Rab5: counterparts with similar function in the early endocytic pathway. *Journal of Cell Science* **108,** 3509–3521.

Sohn EJ, Kim ES, Zhao M, *et al.* 2003. Rha1, an Arabidopsis Rab5 homolog, plays a critical role in the vacuolar trafficking of soluble cargo proteins. *The Plant Cell* **15,** 1057–1070.

Stenmark H, Parton RG, Steele-Mortimer O, Lutcke A, Gruenberg J, Zerial M. 1994. Inhibition of rab5 GTPase activity stimulates membrane fusion in endocytosis. *EMBO Journal* **13,** 1287–1296.

Tse YC, Mo B, Hillmer S, Zhao M, Lo SW, Robinson DG, Jiang L. 2004. Identification of multivesicular bodies as prevacuolar compartments in Nicotiana tabacum BY-2 cells. *The Plant Cell* **16,** 672–693.

Ueda T, Yamaguchi M, Uchimiya H, Nakano A. 2001. Ara6, a plant-unique novel type Rab GTPase, functions in the endocytic pathway of Arabidopsis thaliana. *EMBO Journal* **20,** 4730–4741.

Vernoud V, Horton AC, Yang Z, Nielsen E. 2003. Analysis of the small GTPase gene superfamily of Arabidopsis. *Plant Physiology* **131,** 1191–1208.

Wang H, Zhuang XH, Hillmer S, Robinson DG, Jiang LW. 2011. Vacuolar sorting receptor (VSR) proteins reach the plasma membrane in germinating pollen tubes. *Molecular Plant* **4,** 845–853.

Wang J, Cai Y, Miao Y, Lam SK, Jiang L. 2009. Wortmannin induces homotypic fusion of plant prevacuolar compartments. *Journal of Experimental Botany* **60,** 3075–3083.

Wang J, Ding Y, Hillmer S, Miao Y, Lo SW, Wang X, Robinson DG, Jiang L. 2010. EXPO, an exocyst-positive organelle distinct from multivesicular endosomes and autophagosomes, mediates cytosol to cell wall exocytosis in Arabidopsis and tobacco cells. *The Plant Cell* **22,** 4009–4030.

Wang J, Li Y, Lo SW, Hillmer S, Sun SS, Robinson DG, Jiang L. 2007. Protein mobilization in germinating mung bean seeds involves vacuolar sorting receptors and multivesicular bodies. *Plant Physiology* **143,** 1628–1639.

Wang J, Shen J, Cai Y, Robinson DG, Jiang L. 2013. Successful transport to the vacuole of heterologously expressed mung bean 8S globulin occurs in seed but not in vegetative tissues. *Journal of Experimental Botany* **64,** 1587–1601.

Wegner CS, Malerod L, Pedersen NM, Progida C, Bakke O, Stenmark H, Brech A. 2010. Ultrastructural characterization of giant endosomes induced by GTPase-deficient Rab5. *Histochemistry and Cell Biology* **133,** 41–55.

Woollard AA, Moore I. 2008. The functions of Rab GTPases in plant membrane traffic. *Current Opinion in Plant Biology* **11,** 610–619.